Mol Neurobiol (2017) 54:2483–2496
DOI 10.1007/s12035-016-9836-z

Mechano-Transduction Signals Derived from Self-Assembling Peptide Nanofibers Containing Long Motif of Laminin Influence Neurogenesis in In-Vitro and In-Vivo

Shima Tavakol[1,2,3] · Sayed Mostafa Modarres Mousavi[4] · Behnaz Tavakol[5] · Elham Hoveizi[6] · Jafar Ai[7,8] · Seyed Mahdi Rezayat Sorkhabadi[1,9,10,11]

Received: 8 January 2016 / Accepted: 4 March 2016 / Published online: 16 March 2016

Abstract Astroglial scaring and limited neurogenesis are two problematic issues in recovery of spinal cord injury (SCI). In the meantime, it seems that mechanical manipulations of scaffold to inhibit astroglial scarring and improve neurogenesis is worthy of value. In the present investigation, the effect of nanofiber (gel) concentration as a mechanical-stimuli in neurogenesis was investigated. Cell viability, membrane damage, and neural differentiation derived from endometrial stem cells encapsulated into self-assembling peptide nanofiber containing long motif of laminin were assessed. Then, two of their concentrations that had no significant difference of neural differentiation potential were selected for motor neuron investigation in SCI model of rat. MTT assay data showed that nanofibers at the concentrations of 0.125 and 0.25 % *w/v* induced higher and less cell viability than others, respectively, while cell viability derived from higher concentrations of 0.25 % *w/v* had ascending trend. Gene expression results showed that noggin along with laminin motif over-expressed TH gene and the absence of noggin or laminin motif did not in all concentrations. Bcl_2 over-expression is concomitant with the decrease of nanofiber stiffness, NF^+ cells increment, and astrogenesis inhibition and dark neuron decrement in SCI model. It seems that stiffness affects on Bcl_2 gene expression and may through β-Catenin/Wnt signaling pathway and BMP-4 inhibition decreases astrogenesis and improves neurogenesis. However, stiffness had a significant effect on upregulation of $GFAP^+$ cells and motor neuron recovery in in vivo. It might be concluded that eventually there is a critical definitive point concentration that at less or higher than of it changes cell behavior and neural differentiation through different molecular pathways.

Keywords Neurogensis · Mechano-transduction · Self assembling pepetide · Nanofiber · Laminin

✉ Shima Tavakol
shima.tavakol@yahoo.com

✉ Jafar Ai
Jafar_ai@tums.ac.ir

✉ Seyed Mahdi Rezayat Sorkhabadi
rezayat@tums.ac.ir

[1] Department of Medical Nanotechnology, School of Advanced Technologies in Medicine, Tehran University of Medical Sciences, Tehran 1417755469, Iran

[2] Drug Nanocarriers Research Core, Razi Drug Research Center, Iran University of Medical Sciences, Tehran, Iran

[3] Student's Scientific Research Center, Tehran University of Medical Sciences, Tehran, Iran

[4] Shefa Neuroscience Research Center, Khatam Alanbia Hospital, Tehran, Iran

[5] School of Medicine, Kashan University of Medical Sciences, Kashan, Iran

[6] Department of Biology, Faculty of Sciences, Shahid Chamran University of Ahvaz, Ahvaz, Iran

[7] Department of Tissue Engineering, School of Advanced Technologies in Medicine, Tehran University of Medical Sciences, Tehran, Iran

[8] Brain and Spinal Injury Research Center, Imam Hospital, Tehran University of Medical Sciences, Tehran 1417755469, Iran

[9] Department of Toxicology and Pharmacology, School of Pharmacy, Pharmaceutical Sciences Branch, Islamic Azad University (IAUPS), Tehran, Iran

[10] Experimental Medicine Research Center, Tehran University of Medical Sciences, Tehran, Iran

[11] Department of Pharmacology, School of Medicine, Tehran University of Medical Sciences, Tehran, Iran

Introduction

Spinal cord injury (SCI) due to switch on anti-growth pathways and insufficient neurogenesis is one the most problematic disorders in clinic and has been not find a procedure or medicine that completely recover it. Based on a clinical epidemiology on incidence of SCI, it has been reported that men, younger than 30 years old more experience SCI as compared to women and its common cause is traffic accident [1]. Based on WHO fact sheet on 2013, it is estimated that annually approximately 250000 and 500000 people suffer from SCI [2]. In this regard, investigating a medicine or scaffold that inhibits astroglial scarring and induces neurogenesis would be worthy of value. However, nervous system changes mechanical properties based on its developmental stage and location [3], and it is the reason of transition from neurogenesis to geliogenesis concomitant with stiffness of the brain with age in some cases. In fact, it got stiffened with age [3].

It is interesting to mention that although elastic modules of brain tissue is in the range of 500 Pa [4] and a higher for spinal cord due to blood vessels and longitudinal alignment of axons, the neural stem and progenitor cells in these tissues naturally live in a soft substrate that do not bear any load due to supportive effect of cranium and vertebrae while they response to mechanical stimuli [5]. In fact, neural cells have potential to change its genotype and phenotype in face to mechano-transduction signals. Researchers disclosed that elastic modules of 10 Pa [6] and higher than 10 KPa [4] are not favor for neural proliferation and differentiation; however, stiffer matrix with elastic modules in a range of 100–500 Pa and higher than 1000 Pa is favor for neural and glial cells, respectively [6, 7]. Leipzig et al. demonstrated that elastic modules of 7 and less than 1 and 3.5 KPa are favor for oligodendrocyte and astrocyte differentiation, respectively [4]. While others indicated that matrix with elastic modules of 9 KPa induces astrocyte differentiation [8]. However, oligodendrocyte maturation happens in soft substrate with less than 1 Pa elastic modules [4]. Alteration of tension and stiffness of a scaffold as ECM mimicking biomaterial influences conformation and spatial presentation of integrin and its ligands, respectively that resulted in change of their affinity together. All together are caused changes in expression of transcription factors and chromatin remodeling enzymes (tension-induced proteins) [9] that resulted in different response together [7]. Some molecular pathways involved in mechanical stimulation are summarized in the following.

It was revealed that substrate stiffness in the tensioned state is in good agreement with α5β1-fibronectin adhesive bonds (catch bond), and formation of tensioned bonds triggers downstream signaling pathways same as actin-myosin II and afterwards phosphorylation of focal adhesion kinases (FAK Y397) [10]. Then, microtubule is necessary to transmit stress to cytoplasmic proteins same as src [11]. Src localizes in endosomal membrane adjacent to microtubules [12, 13]. To rapidly activate src in the deep of cytoplasm, actin and myosin II are necessary. However, extent of microtubule deformation and displacement defines degree of src activation [11]. Tension influences on mechano-sensitive ion channels that transduce external tension to cells via Ca^{2+} signaling pathway, as well [14, 15]. Besides, integrin directly through the activation of cAMP signaling pathway triggers protein synthesis machinery [3, 16].

By regards to this fact that mechano-transduction signals define in part fate of stem or progenitor cells towards neuron or astroglial cells through non-muscle myosin II [17], actin and focal-adhesion structures [18], so matrix stiffness is key factor in designing of hydrogel-based scaffold for inhibition and induction of astroglial scarring and neurogenesis, respectively. It is notable that a pre-committed cell to a specialized matrix stiffness is less selective for inductive effect of a chemical inducer [18].

Besides elastic modules, epitope concentration influences cell behaviors [19]. It is demonstrated that when the space of RGD ligands be in the length of less than 70 nm (higher density of RGD ligands) [20], so an integrin cluster (at least 4 integrins) with approximately 200 nm space to adjacent cluster [21] along with doughnut-shaped structures in the length of 25 nm in diameter is formed. These processes resulted in a strong cell adhesion with bigger focal adhesion complex and improved actin polymerization as compared to the lower density [22]. However, integrin ligand density should not be exceeded more than a definitive quantity [23]. Even thought weak cell adhesion may conduct cells to apoptosis pathways [20]. It is notable that, decrease of scaffold's stiffness with dilution of its biological substance such as laminin and Matrigel [24] will decrease ligand density of integrin binding site. So applying of their epitope in the scaffold structure will solve this issue [25, 26].

Laminin (900 kDa) is one the most important proteins of ECM with diversified capacity associated with its specific motifs (IKVAV and YIGSR). It is disclosed that IKVAV motif as a 208th sequence of laminin-1 α1 chain [27, 28] more preferentially involves in neurite outgrowth [29, 30], neural adhesion, and differentiation [31] than YIGSR motif. IKVAV through α3ß1, α4ß1, and α6ß1 integrin sites is bound to integrin [28, 32, 33]. However, laminin through activation of ERKs, JNK, and PI3K/Akt signal pathways regulates neural proliferation and differentiation [34–36].

Ortinau et al. mixed laminin with $(RADA)_4$ as a self-assembling core and investigated proliferation and differentiation of human neural progenitor cells at different concentrations and compared them with 2D cell cultures. Their results showed no difference between cell viability and Tuj-1 upregulation at different concentrations (0.15, 0.25, and 0.5 %). However, TH had been up and downregulated at the concentrations of 0.25 and 0.5 %, respectively [37]. Besides, they

emphasized that they did not investigate the effect of stiffness in neural proliferation and differentiation.

Since physical entrapment of adhesive motifs into 3D scaffold boosts its biological capacity [19], and also, $(RADA)_4$ sequence is undergone ß sheet and nanofiber structure upon face to ionic environment, so the laminin sequence was attached to the $(RADA)_4$ sequence via 2 glycines. This assimilated structure of ECM along with its hydrogel form is critical for recovering of CNS. Although, there are a number of investigations that have proved higher neural proliferation and differentiation potential of $(RADA)_4$-IKVAV as compared to $(RADA)_4$ through the ERK signal pathway [38, 39] but it has been disclosed that as a point of view a cellular responses improvement, laminin with long motif (CQAASIKVAV) is superior to shorter ones (IKVAV or SIKVAV) [40]. Lévesque and Tavakol et al. proved neurite outgrowth capacity of CQAASIKVAV hydrogels, as well [41–43].

Gelain et al. disclosed that the number of amino acids as an anchoring spacer, glycine, alters neural signal transduction, and then, neural differentiation. In fact, 0 glycine spacer induced higher stiffness to the structure as compared to 2 and 4 glycine spacers, and this stiffness dose not well support neural adhesion and proliferation. They indicated that there is no significant difference between percentages of β-Tubulin$^+$ and GalC/O4$^+$ cells derived from NSC treated with 2 and 4 glycine spacers. Nevertheless, 2 spacers provoke less reactive astrocyte in comparison with 4 glycines [44]. Based on these information, in this study, to decrease reactive astrocytes and afterwards astroglial scar decrement in the site of injury, long motif of laminin anchored via 2 glycines to self-assembling peptide core and human endometrial-derived stromal cells (hEnSCs) was selected a source of multipotent stem cells that are differentiated towards neural cells. These cells are derived from the endometrium of human and have adipo, chondro, and osteo differentiation capacity [45]. HEnSCs in comparison with other stem cell types have disclosed some profits that makes them significant source for cell therapy. Some benefits are immunosuppressive ability [46], higher doubling time (19.4 h) and clonogenicity (1.25 %) as compared to UCBSC, and not disclosed teratoma improvement unlike embryonic stem cells [47–49]. However, FDA approved hEnSC transplantation in human [50].

In our previous study, the neural differentiation potential of hEnSCs encapsulated into Ac-$(RADA)_4$GGCQAASIKVAV-$CONH_2$ (R-CQIK) and supplemented with Noggin was investigated at the 0.125 concentration and was named 0.125 [42]. In the present study, it is aimed to assess neural differentiation potential of R-CQIK at 0.125, 0.25, and 0.5 % *w/v* concentrations (0.125, 0.25, and 0.5) without Noggin. In this study, cells via a sandwich method have been encapsulated into nanofibers [51]. In fact, we are going to investigate whether this nanofiber in the media poor of Noggin will suppress GFAP or not and also investigate the effects of increase of gel concentration (stiffness) in neural differentiation and motor neuron recovery, in vitro and in vivo. To the best of our knowledge, the present study is the first mechano-transduction investigations of R-CQIK nanofiber using hEnSC in in vitro and in vivo, respectively.

Materials and Methods

Oligopeptide Characterization by Reverse Phase HPLC

The oligopeptide was synthesized via solid-phase synthesis method and then oligopeptide purity reverse phase HPLC was performed.

HEnSCs Isolation and Analysis

HEnSCs were isolated from a healthy 28-year-old woman in accordance with the Tehran University of Medical Sciences ethical committee law. The isolation method and analysis have been reported in our previous study [52]. Briefly, the endometrial tissue washed with Hank's balanced salt solution rich 1 % penecterep (Gibco, USA), then was dissected with collagenase I (1 mg/ml; Gibco, USA), passed through sieves 3 times and finally using Ficoll-Paque (Sigma, USA), mononuclear cell was separated. After the third passage, cells seeded in Dulbecco's modified Eagle's medium/F12 (DMEM/ F12) medium (Gibco, USA) containing 10 % fetal bovine serum (FBS; Gibco, USA), 1 % antibiotic, and 1 % glutamine (Gibco, USA) were prepared for flow cytometry. The investigated cell surface marker was CD146 (endometrial stem cell marker), CD105 (endoglin), CD90 (mesenchymal markers), CD34 (hematopoietic marker), and CD31 (endothelial marker).

Self-Assembled Nanofiber Formation

R-CQIK powder was dissolved in deionized water (Mili Q water) at the concentration of 1 %. Then, it was sonicated for 30 min before well-plate coating and cell encapsulation. One hundred microliters of oligopeptide solution was eluted in neural differentiation media (NPBM, bFGF, EGF, and NSF-1 (LONZA), BDNF (50 ng/mL) (Sigma), 1 % antibiotic and 2 mM glutamine) at the concentration of 0.125 % (gr/ml), it was gently added to pre-coated plate and allowed to from nanofiber 3 h. After well-plate coating, hEnSCs (4×10^3) were encapsulated into R-CQIK solution at the concentrations of 0.125, 0.25, and 0.5 % *v/w*. Encapsulated hEnSCs in -CQIK nanofibers were incubated at 37 ° C in 5 % CO2 and 95 % moisture.

DPPH Assay

1, 1-Diphenyl-2-picryl-hydrazyl (DPPH) with an unpaired valence electron has free radical scavenger potential and was applied as antioxidant assay. It was purchased from Sigma–Aldrich (USA) and diluted in methanol (100 μM). -CQIK at the final concentrations of 0.125, 0.25, and 0.5 % *v/w* were diluted in methanol to decrease acidic pH of oligopeptide solution. One hundred microliters of 100 μM solution of DPPH in methanol was added to 100 μl of nanofiber solution and was kept in 30 °C for 30 min, and the absorbance was measured using Eliza reader at 517 nm (Fisher Lifesciences).

MTT Assay

MTT (3-(4, 5-dimethylthiazol-2-yl)-2, 5 diphenyltetrazolium bromide) assay measures succinate dehydrogenase enzyme activity as a marker of mitochondrial function. HEnSCs (1×10^4 cells/ml) encapsulated triplicate into 0.125, 0.25, 0.5, and 1 nanofibers for 48 h. After incubation time, medium was removed, and cells were treated with 100 μl of 5 mg/10 ml MTT solution for 4 h. To dissolve hydrazine crystal, dimethyl sulfoxide (DMSO; Sigma, USA) was added and then, absorbance was read at 570 nm using ELIZA reader (Fisher Lifesciences) up to 20 min. To eliminate dye absorbance derived from protein, background group added to the analysis groups. BE(2)-M17 viability has been reported in our previous report [25].

Study of Cell Membrane Damage

Lactate dehydrogenase (LDH), a cytoplasmic enzyme, assay was performed to study the cell membrane. When cell membrane is faced to the toxic material, it induces cell membrane damage and leakage. So LDH is released to the extracellular environment. Clonal human neuroblastoma (BE(2)-M17) cell line at a final concentration of 1×10^4 cells/ml was encapsulated triplicate into 0.125, 0.25, and 0.5 nanofibers in RPMI medium poor of FBS and pyruvate (pyruvate induces false positive in LDH assay) supplemented with 1 % antibiotic penicillin/streptomycin (Gibco, USA) for 24 h. After the incubation time, 96-well plates were centrifuged and 100 μl/well was mixed with 100 μl of reaction mixture for 30 min at 22 ° C. Absorbance was read in triplicate at 490 nm in 96-well format using ELIZA reader (Fisher Lifesciences).

Neural Differentiation

HEnSCs in passage three was induced to neural differentiation for 21 days. hEnSCs were encapsulated into 0.125, 0.25, and 0.5 nanofibers and incubated in medium consisting NPBM, bFGF, EGF, NSF-1, BDNF (50 ng/ml), 1 % antibiotic, and 2 mM glutamine for remained time. Encapsulated hEnSCs in peptide nanofiber were imaged under an inverted light microscope (Olympus AX-800) equipped with a digital camera (Leica, DC200) at 3, 7, 10, and 18 days post-induction.

Immunocytochemistry (ICC)

Twenty-one days post-treatment, the cells underwent cell marker evaluation via immunostaining for the following markers, Nestin (1:200; Chemicon), Tuj-1 (1:500; Abcam), and GFAP (1:30; Abcam) and neurofilament (NF; 1:100; Abcam). Briefly, cells were washed, fixed and permeabilized and blocked in 4 % paraformaldehyde, 0.1 % Triton X-100, 0.1 % human serum albumin (HSA) in PBS, respectively. Then, they were incubated with primary antibody in 4 °C overnight. Afterwards, anti-goat FITC-conjugated as a secondary antibody and DAPI satin as nuclear staining were added to cells for 1 h and 30 s at room temperature, respectively. For negative controls, first antibodies were omitted.

Quantitative Polymerase Chain Reaction (Real-Time PCR)

To quantify the difference between the mRNA levels of neurogenic markers, Nestin, Tuj-1, NF, microtubule-associated protein 2 (MAP2), tyrosine hydroxylase (TH), gamma aminobutyric acid (GABA), glial fibrillary acidic protein (GFAP), oligodendrocyte transcription factor 2 (Olig2), and B-cell lymphoma 2 (Bcl2) as antiapoptotic marker in neuron-like derived hEnSCs encapsulated into nanofibers, real-time PCR was performed. β-actin gene was selected as housekeeping gene. The primers sequences have been mentioned in our previous report [49]. Relative fold change gene expression was investigated on neural differentiated hEnSCs into R-CQIK nanofibers after 21 days post-treatment. The total RNA was extracted, DNase I treatment was applied and random hexamer primed complementary DNA (cDNA) synthesis was carried out using a TAKARA cDNA synthesis kit (Burlington, Japan). CDNA was used for 45 cycle PCR in Rotor-gene Q real-time analyzer (Corbett, Australia) using Maxima SYBR Green Master Mix (Fermentas). Each reaction was repeated three times, and relative fold change gene expression was quantified using the DDCt method.

Morphology Observation of Nucleolus

4',6-Diamidino-2-phenylindole (DAPI) staining was carried out to investigate chromatin nucleus staining as DNA fragmentation in hEnSCs encapsulated into 0.125, 0.25, 0.5, and 1 nanofibers after 48 h. Cells were washed in cold PBS. They were fixed in 4 % paraformaldehyde, then DAPI was added and left for 15 s and was then washed in PBS. Images were recorded using an inverted fluorescence microscope

(Olympus AX-800) equipped with digital camera (Leica, DC200).

In Vivo Study

The chronic moderate spinal cord injury (SCI) induced in 12 male Wistar rats (25–280 g) using weight compression method [53]. All procedures were performed in accordance with the institutional guidelines of the Tehran University of Medical Sciences for animal care and use. Rats were randomly and equally divided in treatment (0.125 and 0.25) and control groups. In this study, due to similarity of neural gene and protein expression of 0.125 and 0.25 nanofibers, they were choosen for further investigation in vivo. Briefly, anesthesia was induced by ketamine (80 mg/kg, i.p.) and xylazine (10 mg/kg, i.p.). After laminectomy at T10 (spinal T9) level, a 35-g weight (with a concave shape tip and an area of 6.6 mm^2) compressed the intact dura for 15 min. After injury, the muscles and skin were sutured, and the animal was hydrated and injected intraperitoneally and intramuscularly with 1 ml lactated Ringer's solution and 6 mg/kg gentamicin, respectively. Antibiotic injection was given daily for 5 days post-surgery. Animals received manual bladder expression twice daily until bladder function was restored within 2 weeks post-injury. In the tenth day post-surgery, animals again were anesthetized, and the spinal cord was re-exposed, then 10 μl of oligopeptide solution in 10 % sucrose (0.125 and 0.5 % *v/w*) was injected into the spinal cord at the lesion epicenter (0.5 mm from the midline and 1.5 mm down from the dura) with the rate of 0.5 μl/min using a 26-gage Hamilton syringe. The same postsurgical treatments were administered as after the initial surgery.

Behavioral Analysis

Recovery of hind limb stepping movements was evaluated by Basso, Beattie, Bresnahan (BBB) open-field locomotor test in which the scores range from complete paralysis (score 0) to normal locomotion (score 21) [54]. Rat was placed in a plexiglas circular apparatus (107-cm diameter, 60-cm wall height) with a nonslip floor. The motor activity of the rat was recorded by a portable camera for 4 min. Then, hind limbs movements were assessed by an observer blinded to the treatment protocol, and BBB scores were averaged from both hind limbs. Only animals with a BBB score of a maximum 1 on day 1 post-injury were included in all further analyses. The test was carried out on day 42 post-injury.

Tissue Preparation and Staining

Forty-two days following injury, the animals were perfused and fixed with 4 % paraformaldehyde in 0.1 M PBS and the subject segment was dissected. Transverse sections (7-μm thickness) were prepared from the paraffin-embedded spinal cords and stained with 1 % cresyl violet (Nissl-staining) and luxol fast blue (LFB). Finally, the sections were dehydrated through a graded series of ethanol and xylene and covered with coverslips.

Immunohistostaining (IHC)

The expression of the NF and GFAP proteins were evaluated through the transverse sections using IHC method. Briefly, the specimens were permeabilized and blocked with PBS/0.3 % TritonX-100/10 %, and BSA 1 %, normal goat serum (NGS) for 1 h at room temperature, respectively. Then slices were incubated overnight with the following primary antibodies diluted in PBS/0.3 % BSA: Mouse anti NF150 (Abcam) for axons and anti GFAP (Abcam) for astrocytes. Goat anti-Mouse Alexa 488 (Molecular Probes, 1:750) and Alexa 594 (Molecular Probes, 1:750) secondary antibodies diluted in PBS/0.3 % BSA were used for signal detection by incubating slices for 1 h. Cell nuclei were counterstained with DAPI (Roche).

Statistical Analysis

Graph pad software was applied to calculate and analyze LDH release, cell viability, relative fold change gene expression of cells encapsulated into different R-CQIK concentrations, and BBB score of animals. Experiments were performed as mean values ± SD or SEM. One-way ANOVA and unpaired *t* test with Welch correction were used for statistical analysis. A *P* value of less than 0.05 was considered statistically significant.

Results

Purity of Oligopeptide and DPPH Assay

The data related to purity of oligopeptide and DPPH assay were reported in our earlier study [49]. In brief, data confirmed oligopeptide's purity and no significant difference between production of H^+ ions in 0.125 and 0.25 nanofibers. However, production of H^+ ions by 0.5 nanofiber was higher than others. It is noticeable that G modules of 0.125, 0.25, and 0.5 % *w/v* of $(RADA)_4$ are 120, 350, and 1480 Pa, respectively, by rheometer instrument.

Cell Morphology and Viability

Cell morphology was tracked using inverted light microscopy for 18 days post-incubation. Figure 1b showed the neural differentiation of encapsulated hEnSCs into nanofibers at different concentrations. It is observed that -nanofibers induced hEnSCs' transformation to neural like cells after 10 days post-incubation.

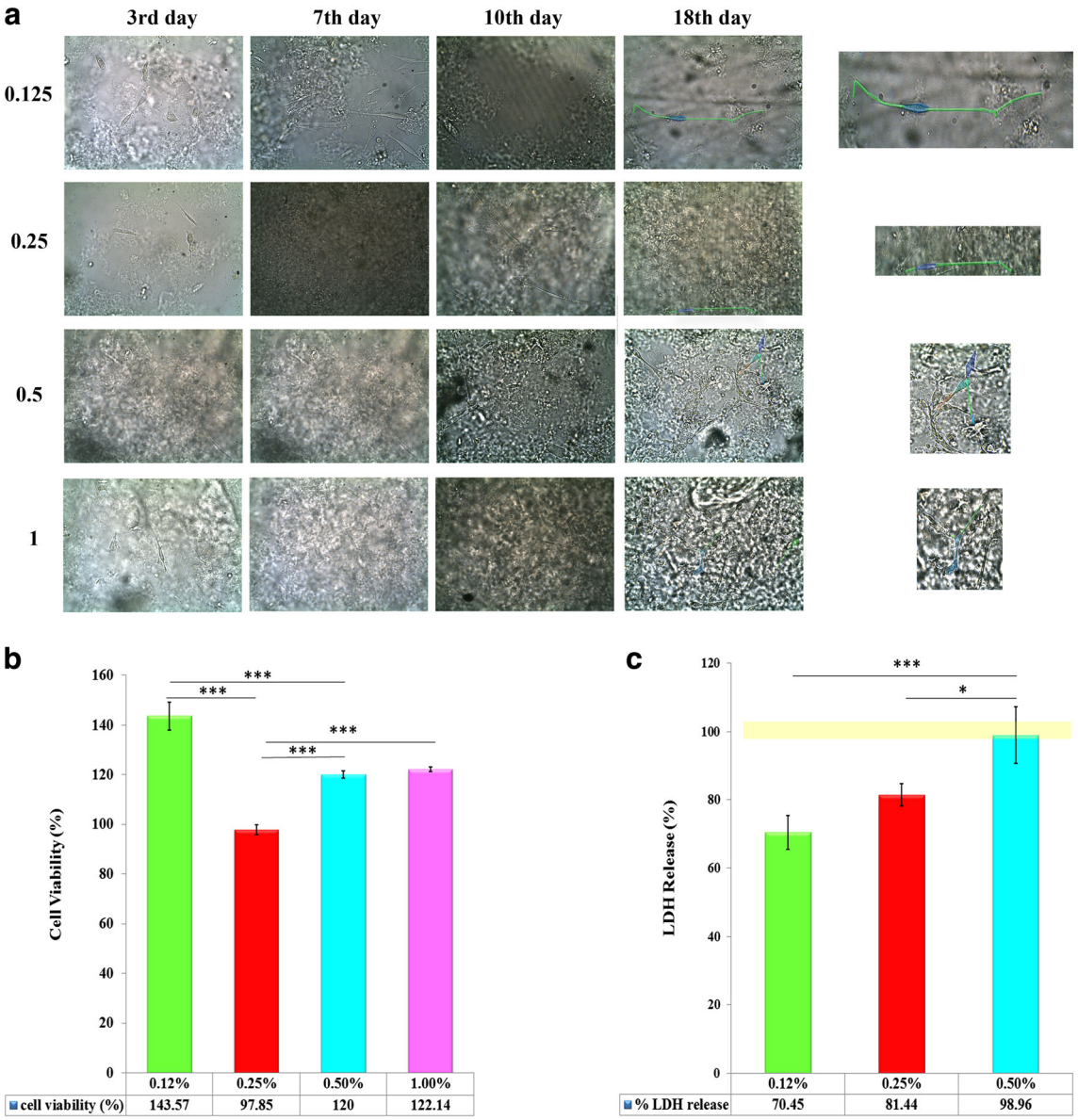

Fig. 1 **a** The morphology of encapsulated hEnSC at different concentration of nanofibers (0.125, 0.25, 0.5, and 1 % *w/v*) imaged under an inverted light microscope (Olympus AX-800) equipped with a digital camera (Leica, DC200) at 3, 7, 10, and 18 days post induction. Cells began to extend their neurite in the morphology of neuron like cells. And The *scale bar* is 50 μm. **b** Viability of hEnSCs encapsulated into nanofibers at 0.125, 0.25, 0.5 and 1 % w/v concentrations after 48 h. 0.25 nanofiber induced highr cell mortality than others however all nanofibers not induced higher cell mortality than 2D cell cultures and induction cell viability of nanofiber more stiffer than 0.25 nanofiber had ascending trend. **c** Percentage of LDH release from BE(2)-M17 cellS encapsulated BE into nanofibers at 0.125,0.25, 0.5 % *w/v* concentrations after 24 h. The % of LDH release had ascending trend with increase of concentration. The *yellow bar* showed 2D cell culture group. *$P < 0.05$; **$P < 0.01$

Although, cells encapsulated into 0.5 nanofiber had higher neural-like cells morphology with extend neurite outgrowth than others on the 18th day post-incubation but their cell mortality after the 18th day was significant higher than 0.125 and 0.25 nanofiber and almost all cells encapsulated into 1 nanofiber died on the 21st day (Fig. 1a).

MTT was done to investigate cell viability of hEnSCs encapsulated in nanofibers on reduction in the mitochondrial metabolic activity (cell respiratory system). Interestingly, results showed that cell viability of hEnSCs encapsulated into 0.125 nanofiber was extremely significant higher than nanofiber at the other concentrations and the control group ($P < 0.001$). However, cell viability of hEnSCs encapsulated into 0.5 nanofiber drastically increased and was significantly higher than 0.25 nanofiber and the control group (Fig. 1b).

LDH Release

LDH release was assessed as a sign of damage to cell membrane. Results showed that nanofibers at different

concentrations induced significantly less or equal cell membrane damage as compared to 2D cell culture. In fact, LDH release from the neuroblastoma cells was concomitant with increase of nanofiber concentration. However, 0.5 nanofiber induced significant higher cell membrane damage as compared to 0.125 and 0.25, ones ($P < 0.5$ and 0.01, respectively) in the range of 2D cell culture (Fig. 1c).

ICC of Neuron Markers

Protein expression of markers involved in neural differentiation in in-vitro may be investigated using detection of Nestin, Tuj-1, NF, and GFAP. Results revealed that GFAP was not upregulated in cells at all nanofiber concentrations while there is no significant difference between protein upregulation of Tuj-1 and NF in cells encapsulated into 0.125 and 0.25 nanofibers. However, 0.5 nanofiber significantly induced Tuj-1 upregulation as compared to the others (Fig. 2a).

Real-Time PCR

Quantitative Real-time PCR was performed to assess the relative fold change of gene expression involved in neural differentiation of cells encapsulated into 0.125, 0.25, and 0.5 nanofibers using detection of nestin, Tuj-1, NF, MAP2, TH, GABA, GFAP, Olig2, and Bcl2 over 21 days of induction. RNAs encoded by the neural genes revealed neural differentiation derived from hEnSC encapsulated into -CQIK nanofibers. Although, GFAP, TH, GABA, and Olig2 were absent in all groups but nestin overexpressed in cells encapsulated into 0.5nanofiber. There is no significant difference between expression of Tuj-1 and NF at 0.125 and 0.25 nanofiber while 0.5 nanofiber induced higher and less gene expression of Tuj-1 and NF than others ($P < 0.001$), respectively. There is no significant difference between gene expression of MAP2 in all groups ($P = 0.0787$) (Fig. 2b). While gene expression of Bcl2 in cells drastically and significantly decrease with increment of nanofiber concentration, these data revealed that nanofiber concentration affects neural differentiation pattern of hEnSC, as a progenitor cell (Fig. 3b).

Morphology Observation of Nucleolus

DAPI staining was carried out to evaluate fragmented nucleus via lighter blue chromatin by 0.125, 0.25, 0.5, and 1 nanofibers. Results from DAPI staining showed that 0.5 and 1 nanofibers induced fragmented nucleus with lighter blue chromatin staining while nucleus stain and appearance of cells encapsulated into 0.125 and 0.25 nanofibers were normal (Fig. 3a).

BBB Test

The compression model was used as an animal model in SCI owing to similarity to actual SCI. Evaluation of functional motor recovery after spinal cord compression using BBB scores showed a final score of 13.75, 8, and 2 in the 0.125, 0.25 nanofibers, and the control groups at the 42nd day post-injury, respectively. The BBB score of 0.125 group had ascending trend and there was significant difference with the scores of 0.25, and the control groups on the 42nd day ($p < 0.001$). Howbeit, there was significant difference between the scores of 0.25 nanofiber and control groups by 42sd day post-implantation. The results revealed that concentration of nanofibers significantly affects motor neuron recovery in rats even with non-significant neural differentiation potential in in-vitro.

Histological Observation

Following implantation of nanofibers in SCI model of rat, a significant larger cavity remained in the dorsal part of injury site when implanted with 0.25 nanofibers as compared to the 0.125 ones on the 42nd day (Fig. 4b). However, it was observed extensive tissue repair including cellular recovery and axonal myelination (blue spot) by low concentration's nanofiber groups compared to higher ones. The axonal myelination was far from the cavity in the 0.25 nanofiber while it was adjacent to the smaller cavity of implanted 0.125 nanofibers. Albeit, there was no significantly difference between myelination and cavity size of higher concentration of nanofiber as compared to control group may be due to high extent of reactive astrocytes and non-inhibition of them in the injury site (Fig. 4b).

Moreover, Nissl staining disclosed abundant number of dark neurons (25–27) in the SCI model implanted with 0.25 nanofiber as compared to 0.125, ones (1–2) (Fig. 3c). It seems that low nanofiber concentrations that exhibited lesser stiffness to the environment induced supportive effects as compared to stiffer ones. The Nissl and LFB staining revealed a strong secondary response in rats implanted with stiffer scaffold.

IHC of Neural Markers

There is significantly difference between up- and downregulation of NF and GFAP markers in two groups of nanofibers. Following 42 days post-implantation of chronic SCI model, NF marker was abundant around the injury site which implanted with 0.125 nanofiber as compared to stiffer ones. This finding disclosed higher quantity of axon regeneration around the cavity implanted with lesser stiffness nanofiber as compared to higher stiffness group. However, the story was completely different about the GFAP marker, and it was

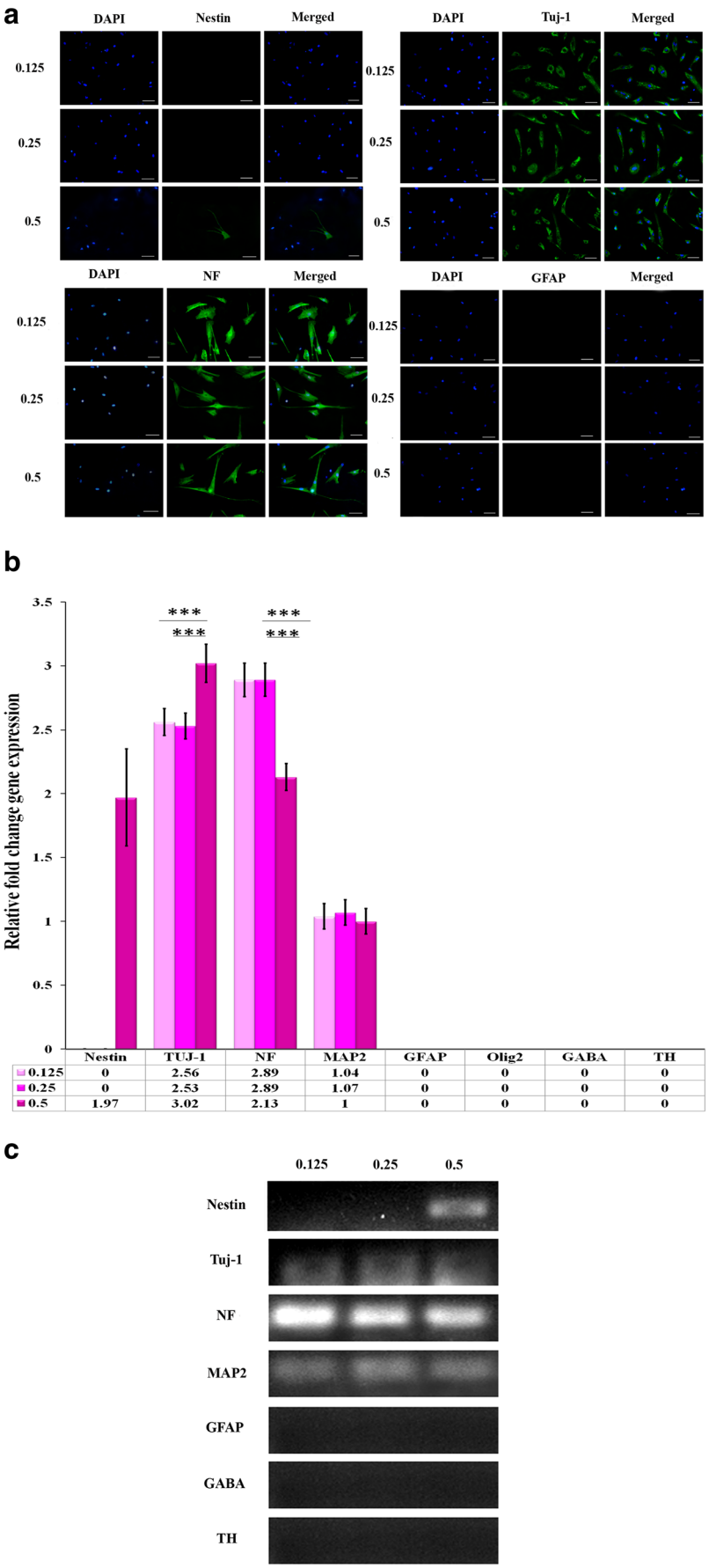

Fig. 2 **a** The upregulation of Nestin, Tuj-1, NF, and GFAP markers in hEnSCs encapsulated into nanofibers by ICC method. All nanofiber suppressed GFAP up-regulation. The *scale bar* is 50 μm. **b** Neural gene expression analysis of hEnSCs encapsulated into 0.125, 0.25, and 0.5 nanofibers by real-time RT PCR. Results showed gene over-expression 0.125 and 0.25 nanofiber had no significant difference in neural gene expression of Nestin, Tuj-1, MAP2, and NF markers. However, cells had not expressed GFAP and GABA and TH in all concentrations. ***$P < 0.001$. **c** The RT-PCR figure of neural gene expression induced by 0.125, 0.25, and 0.5 nanofiber confirmed realt-time PCR data

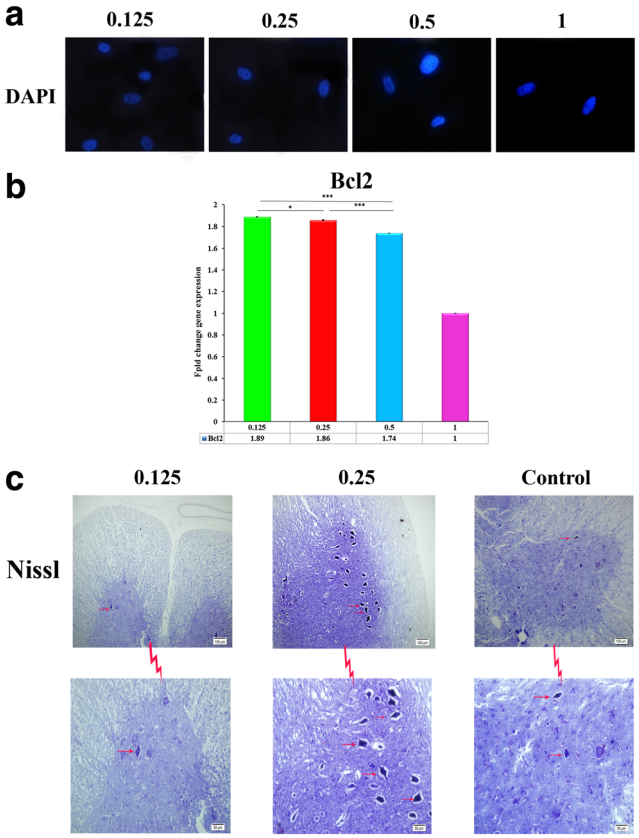

Fig. 3 **a** DAPI staining of cells encapsulated into 0.125, 0.25, 0.5, and 1 nanofibers after 48 h. 0.5 and 1 nanofibers showed more lcells with ighter blue chromatin. **b** Bcl2 gene expression of hEnSCs encapsulated into nanofibers indicated increase of nanofiber concentration had descending trend with Bcl2 gene expression. **c** Nissl staining of specimens from SCI model of rat implanted with 0.125, 0.25, and the control group showed more number of dark neurons in rats implanted with stiff scaffold than softer ones. However, the control group had less and higher dark neurons than 0.25 and 0.125 nanofiber, respectively

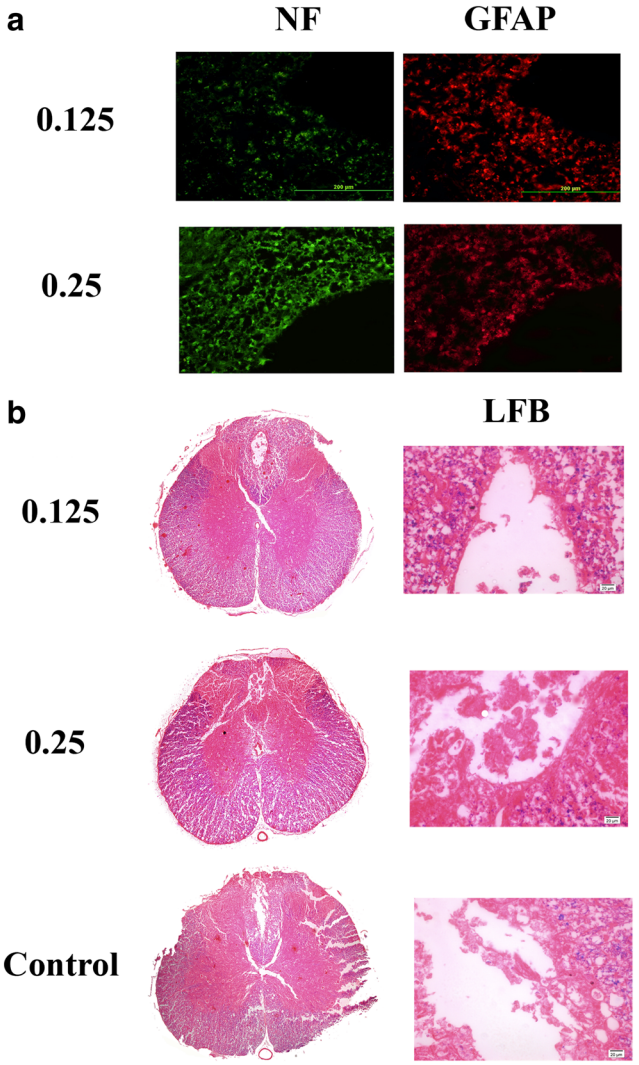

Fig. 4 **a** Investigation of NF and GFAP protein markers around the cavity in SCI model of rat implanted with 0.125 and 0.25 nanofiber using IHC method. The *scale bar* is 200 μm. Results showed up and downregulation of NF and GFAP markers in rat implanted with 0.125 nanofiber as compared to 0.25, ones. **b** LFB stainging of specimens belongs to the rats implanted with 0.125, 0.25 nanofiber and the control group. *Blue dots* indicated laminin staining of neurons. 0.125 nanofiber exhibted higher cavity recovery (*left*) and myelination than others

observed abundant infiltration of $GFAP^+$ cells as a marker of reactive astrocyte around the control (not shown) and the group implanted with stiff scaffold. In fact, lower concentration of nanofiber induced up and down regulation of NF and $GFAP^+$ cells around the cavity, respectively that exhibited extended axon regeneration as compared to higher concentration group (Fig. 4a). Dominancy of astrogenesis in higher concentration of nanofiber (0.25 % *w/v*) proves the potential of mechno-transduction signals in neural differentiation in in vivo.

Discussion

In this study, long motif of laminin at different concentrations was investigated as a view of cell membrane damage, cell viability (mitochondrial function), neural differentiation in vitro, and motor neuron recovery in a SCI model in rat. Results showed that they influenced biologic pathways and organelles in different manners. The present study demonstrated the neurogenesis and anti-astrogliosis potential of this nanofiber in vitro and in vivo. While the 0.125 and 0.25 nanofibers had no significantly neural differentiation potential difference but its concentration had significantly influence in in-vivo model of SCI. Some researchers believed that although stiffness of scaffold has critical role in the fate of cells but it is not sufficient to completely terminate differentiation and some differentiation chemical cues is necessary and applying of both soluble factors and compliance stiffness has synergism effect on cell differentiation [18, 55]. It is notable that downstream signals derived from mechanical and chemical stimuli have some differences for example in the time of signal

transduction [11]. In the present investigation, the motif of laminin was applied as a chemical stimulus. C-terminal of laminin-1 α1 chain is responsible for neurite outgrowth developing, neuronal cell adhesion [56–58], and stimulation of focal adhesion formation [4, 18]. These data proved the usage of α1 chain's motif as a bioactive segment inducing neural differentiating in hEnSCs.

Data from LDH release induced from different concentrations of nanofiber revealed an ascending trend with the concentration increment. However, cell membrane damage still was not significantly higher than the control group and even in cells encapsulated into 0.125 and 0.25 nanofibers were significantly less than control group. Although, data from DPPH assay showed increase of H^+ concentration in environment parallel to increase of nanofiber as compared to the control group due to acidic moiety in oligopeptide structure but the acidic pH did not induce cell membrane damage to cells at all concentrations. It could be related to the supportive effect of scaffolds from damaging effect of H^+ ions on cell membrane. However, at higher H^+ concentration, its supportive potential decreases as low as the control group. It seems that neuroblastoma cell membrane integrity has decreased not only due to H^+ ions but also owing to increase of stiffness at higher concentrations. In fact, neuroblastoma cells that lives in a soft brain tissue sense tension via mechano-transduction signals from integrin sites and afterwards, are triggered conformational change of integrin [10], spatial change of binding ligands in ECM, change of their affinity together [4], clustering of integrin [10, 59, 60], and downstream signaling pathways.

Based on data from MTT assay, it could be said that lower concentration induced higher cell viability than higher ones. Although, 0.25 nanofiber induced a significant less cell viability as compared to the other concentrations, but there was no significant difference as compared to the 2D group. In fact, nanofibers formed a favorable environment for cell viability as compared to the rigid and stiff environment of 2D cell cultures. Leipzig believed that elastic modules of higher than 10 KPa is not favor for neural cell proliferation [4] and in the present investigation due to softness of scaffolds and its special nanotopography (fiber diameter and 3D structure) and adhesive motifs, nanofibers induced higher cell viability.

A hydrogel based nanofiber at the concentration of 0.125 % *w/v* exhibited a jiggle and loose-packed composition with increment of fiber distance and decrement of fiber diameter, less adhesive epitope, and higher level of O_2 pressure than 0.25 nanofiber. Since this analysis repeated more than five times and in all repetitions, 0.25 nanofiber induced less cell viability as compared to others (MTT and light microscopy) so it is worthy of value to find a reason for it. It may be said that eventually a bit increase of epitope or stiffness or decrement level of O_2 pressure had not favored for cell viability and affects on mitochondrial function. Maybe it has been a critical point that less or higher nanofiber's concentration had been favored for cell viability and neural differentiation. Besides, increment of nanofiber concentration resulted in more dense-packed composition, fiber distance decrement and eventually fiber aggregation, so cell viability has been decreased even with higher extent of epitope. Influence of nanotopography and stiffness on cell viability alterations might be related to the change of integrin clustering and other adhesion molecules that lead to change the distribution and number of focal adhesions and cytoskeleton organization (vimentin, F-actin, α and γ-tubulin) [7]. So cells based on tension receive from environment modulate function and maybe in this meanwhile there has a critical point that in above and bottom of this point does not follow a linear behavior and leads to downstream signal changes and afterwards, organelle and cell function. Although we related exhibited increase of cell viability from 0.25 to 0.5 nanofiber to decrease level of O_2 pressure, increase of tension and epitope but the combination of them makes cell responses and even a lot of other mechanisms that are hidden. However, this hypothesis must be checked. Results from neural differentiation after 21 days post-induction showed that 0.5 nanofiber does not thoroughly support survival of encapsulated cells may be due to insufficient diffusion of nutrients or oxygen for extended periods of time.

In the present investigation, cell proliferation had been increased in stiff nanofiber of 0.5 and 1 (1 nanofiber not shown) as compared to the softer ones (0.25 nanofiber). It seems that eventually another mechanism of cell proliferation that is related to Hippo signaling and transcriptional coactivator of YAP and TAZ, had involved. YAP and TAZ are switch on and off on stiff and soft scaffolds that resulted in accumulation of these transcription factors in nucleus and cytoplasm, respectively [61]. YAP/TAZ accumulation in nucleus leads to alteration of gene expression and neural cell proliferation improvement by the binding with TEAD [61, 62]. However, YAP gene expression is inhibited by the expression of basic helix-loop-helix (bHLH) transcription factors (Ascl1 or Neurog2) and then its protein is downregulated via Lats1 and/or Lats2 kinases activation, in fact lats1 triggers YAP phosphorylation that is undergone proteolytic degradation [63]. It might be said that it is another reason that neural differentiation improves in soft scaffolds by the inhibition of YAP-TEAD binding as seen in the present investigation. Another mechanism beside YAP in the role of scaffold stiffness in neural differentiation related to Rho GTPase. It was revealed that Rho A and Cdc42 activated in stiff scaffold as compared to soft ones that suppress neurogenesis and stiffened neural stem cells [64]. Mechanical stimuli affects on neural differentiation by the different pathways. For example, they act by transient receptor potential (TRP) family. It was indicated that canonical TRP channel TRPC1 through Ca^{2+} signaling pathway after an external tension, influences neural differentiation and development. Tension leads to activation

of ion channels and formation of force-stabilized receptor-ligand bonds. [65, 66]. Another mechanism is through integrin and some integrin-actin filament glues and intracellular signaling molecules such as talin and vinculin [3, 67], src and Cas,Crk associated substrate; involved in migration, survival, transformation, and invasion [68, 69].

Neural differentiation analysis by real time PCR, RT-PCR, and ICC showed alterations of response related to the concentration. It disclosed that Nestin as an early marker of neural differentiation remained just in cells encapsulated into 0.5 nanofiber after 21 days post-induction while it was downregulated in softer ones. It eventually related to level of differentiation. It may be said that low concentration's scaffold has more potency in neural differentiation. However, light microscopy of cells encapsulated at the 1 % *w/v* nanofiber concentration had shown higher extent of neurite outgrowth with high cell mortality on the 18th day (data not shown).

When a tension caused pulling of integrin (conformational change shape of integrin) it leads to change of biophysical property of underlying proteins such as microtubules and improves tubulin polymerization in neuron cells [70–72]. Microtubule maturation by the increase of Tuj-1 is responsible for neuron stiffness [73]. Cells encapsulated into of 0.5 nanofibers significantly over-expressed Tuj-1 as compared to others on the 21st day. Although, results of Ortinau investigation [37] revealed no significant difference between Tuj-1 upregulation at different concentrations on the seventh day but increment and decrement pattern of Tuj-1 was similar to the present study. Researchers indicated that soft scaffold with elastic modulus less than 300 Pa induced abundant number of Tuj-1$^+$ cells as compared to 75000 Pa, and this trend had descending manner concomitant with stiffness increment. They indicated this effect is related to less activity of Rho A and Cdc42 in soft matrix. However, the Rac1 activity had not altered in all stiffness, and it seems that in the stiff matrix, activity of Rho A does not influence neuronal differentiation [64]. The inhibition of RhoA/B/C, ROCK, and myosin II in existence of Rho A, increased the level of neuronal differentiation; however, inhibition of MLCK, Src, and FAK had no influence on it [64].

The in vitro and in vivo results of gene expression and protein markers revealed that NF was upregulated in cells encapsulated into or implanted in rats with softer scaffold while stiffer ones induced up-regulation of GFAP$^+$ cell around the cavity of SCI model. Adhesion complex in neurons have point contact and focal adhesion in glial cells [3]. In a compliant scaffold, in our study; 0.125 nanofiber, neurogenesis is a dominant process while in a stiff scaffold gliosis will dominant as seen in elderly people with increase of stiffness in nervous system [3, 69]. It is interesting to note that increase of GFAP leads to tissue stiffing that in return decreases neurogenesis and increases GFAP $^+$ cells [3]. Keung et al. demonstrated that increase of stiffness by 10 KPa increases in ascending manner up-regulation of GFAP$^+$ cells to 20 %. Although approximately 5 % of population was related to MBP$^+$ cells in soft substrate but it was completely suppressed in stiff matrix higher than 1500 Pa. They revealed that increase of GFAP$^+$ cells in stiff matrix is related to activation of Rho A and Cdc42 as a Rho GTPase signaling pathway members [64]. It is notable that inhibition of RhoA/B/C, ROCK, myosin II, src, MLCK, and FAK in existence of Rho decreases the level of GFAP$^+$ cells [64]. Lei et al. disclosed that overexpression of Bcl2 is accommodated with inhibition of astrogenesis [23, 74] and improvement of neurogenesis [75] and axon elongation. Our results showed that with the increase of concentration, the gene expression of Bcl2 has drastically decreased and this finding is concomitant with the upregulation of GFAP$^+$ cells in higher concentration of nanofiber implanted in SCI model of rat. Bcl2 affects through β-catenin signaling pathway on neurogenesis increment and astrogenesis decrement [23]. Also, it seems that stiffness may through activation of b-catenin/wnt and inhibition of BMP-4 signaling pathways improve neurogenesis and inhibit astrogenesis. The effect of GFAP suppression in in vitro via different concentration of laminin was independent from noggin and its inhibition in SCI model of rat is related to trigger of mechanotransduction signaling. Neurons which differentiated in soft scaffolds got stiffer than adjacent glial cells and vice versa [68], so they attract together. Neurons in in vitro cell culture medium grow on the glial cells [10, 68, 69]. They adapt number and length of neurites and their morphology based on stiffness of scaffold in SCI [10, 11].

Besides, NF was overexpressed in soft scaffolds (0.125 and 0.25) as compared to the stiff ones (0.5). This finding is in good agreement with the gene expression of Bcl2. The present study showed that with the increase of stiffness, Bcl2 gene expression has decreased and NF downregulated. There is some studies that disclosed the dependency of Bcl2 gene expression to neurite outgrowth through intracellular Ca^{2+}, CREB, and Erk signaling pathways [76, 77].

Nissl staining showed that with the increase of concentration, dark neurons significantly increase. It seems that most neurons experience apoptosis or damage when the concentration increases. It is in good agreement with the Bcl2 gene expression data in in vitro. Wang et al. reported that Bcl2 gene expression may suppress apoptosis in neurons post-SCI [78]. It is derived that eventually soft scaffold induced overexpression of Bcl2 gene and afterwards it has been observed a few number (1–2) of dark neurons in the region while stiff's scaffold did not support Bcl2 gene over-expression and resulted in abundant number of dark neurons (25–27) in region (it is suggested that is checked).

Based on LFB staining, soft scaffold exhibited higher secretion of myelin derived from oligodendrocyte than stiffer ones. As mentioned before, oligodendrocyte differentiation starts in stiff matrix but its maturation to secrete myelin

continues in soft matrix. It seems that in the present investigation, soft (0.125) scaffold has induced oligodendrocyte maturation and resulted in secretion of myelin^{+} sheets.

In conclusion, based on our data, it might be said that in in vitro investigation of neural differentiation derived from stem cells there is a critical point that less or higher nanofiber's concentration is favor for cell viability and neural differentiation and does not follow a linear behavior and eventually Bcl2 gene expression influences neurogenesis and inhibition of astrogenesis at the concentration manner through mechanotransduction signals. Besides, it seems that accompaniment of noggin and laminin is essential for TH gene expression. Future experiments directed to study of molecular mechanism behind the relationship between Bcl2 gene expression in SCI model of rat and scaffold stiffness and also to investigate more stiff scaffolds (higher concentration) with this nanofiber in the SCI model of rat.

Acknowledgments This work was supported by grant from the Iran National Science Foundation (INSF) for the financial support (grant number 92022532) and Tehran University of Medical Sciences, Iran.

Compliance with Ethical Standards All procedures were performed in accordance with the institutional guidelines of the Tehran University of Medical Sciences for animal care and use.

References

1. Singh A, Tetreault L, Kalsi-Ryan S, Nouri A, Fehlings MG (2014) Global prevalence and incidence of traumatic spinal cord injury. Clin Epidemiol 6:309
2. WHO (November 2013) Spinal cord injury
3. Riveline D, Zamir E, Balaban NQ, Schwarz US, Ishizaki T et al (2001) Focal contacts as mechanosensors externally applied local mechanical force induces growth of focal contacts by an mdia1-dependent and rock-independent mechanism. J Cell Biol 153: 1175–1186
4. Leipzig ND, Shoichet MS (2009) The effect of substrate stiffness on adult neural stem cell behavior. Biomaterials 30:6867–6878
5. Mazuchowski EL, Thibault LE. (2003) Biomechanical properties of the human spinal cord and pia mater
6. Saha K, Keung AJ, Irwin EF, Li Y, Little L et al (2008) Substrate modulus directs neural stem cell behavior. Biophys J 95:4426–4438
7. Guilak F, Cohen DM, Estes BT, Gimble JM, Liedtke W et al (2009) Control of stem cell fate by physical interactions with the extracellular matrix. Cell Stem Cell 5:17–26
8. Georges PC, Miller WJ, Meaney DF, Sawyer ES, Janmey PA (2006) Matrices with compliance comparable to that of brain tissue select neuronal over glial growth in mixed cortical cultures. Biophys J 90:3012–3018
9. Jakkaraju S, Zhe X, Pan D, Choudhury R, Schuger L (2005) TIPs are tension-responsive proteins involved in myogenic versus adipogenic differentiation. Dev Cell 9:39–49
10. Friedland JC, Lee MH, Boettiger D (2009) Mechanically activated integrin switch controls α5β1 function. Science 323:642–644
11. Na S, Collin O, Chowdhury F, Tay B, Ouyang M et al (2008) Rapid signal transduction in living cells is a unique feature of mechanotransduction. Proc Natl Acad Sci 105:6626–6631
12. Kaplan KB, Swedlow JR, Varmus HE, Morgan DO (1992) Association of p60c-src with endosomal membranes in mammalian fibroblasts. J Cell Biol 118:321–333
13. Loubéry S, Wilhelm C, Hurbain I, Neveu S, Louvard D et al (2008) Different microtubule motors move early and late endocytic compartments. Traffic 9:492–509
14. Christensen AP, Corey DP (2007) TRP channels in mechanosensation: direct or indirect activation? Nat Rev Neurosci 8:510–521
15. Nilius B, Voets T. Diversity of TRP channel activation; 2004. Chichester; New York; John Wiley; 1999. pp. 140–148
16. Meyer CJ, Alenghat FJ, Rim P, Fong JH-J, Fabry B et al (2000) Mechanical control of cyclic AMP signalling and gene transcription through integrins. Nat Cell Biol 2:666–668
17. Conti MA, Even-Ram S, Liu C, Yamada KM, Adelstein RS (2004) Defects in cell adhesion and the visceral endoderm following ablation of nonmuscle myosin heavy chain II-A in mice. J Biol Chem 279:41263–41266
18. Engler AJ, Sen S, Sweeney HL, Discher DE (2006) Matrix elasticity directs stem cell lineage specification. Cell 126:677–689
19. Silva GA, Czeisler C, Niece KL, Beniash E, Harrington DA et al (2004) Selective differentiation of neural progenitor cells by high-epitope density nanofibers. Science 303:1352–1355
20. Cavalcanti-Adam EA, Aydin D, Hirschfeld-Warneken VC, Spatz JP (2008) Cell adhesion and response to synthetic nanopatterned environments by steering receptor clustering and spatial location. HFSP J 2:276–285
21. Schvartzman M, Palma M, Sable J, Abramson J, Hu X et al (2011) Nanolithographic control of the spatial organization of cellular adhesion receptors at the single-molecule level. Nano Lett 11:1306–1312
22. Cavalcanti-Adam EA, Volberg T, Micoulet A, Kessler H, Geiger B et al (2007) Cell spreading and focal adhesion dynamics are regulated by spacing of integrin ligands. Biophys J 92:2964–2974
23. Dalby MJ, Gadegaard N, Oreffo RO (2014) Harnessing nanotopography and integrin-matrix interactions to influence stem cell fate. Nat Mater 13:558–569
24. Tavakol S, Aligholi H, Gorji A, Eshaghabadi A, Hoveizi E, et al. (2014) Thermogel nanofiber induces human endometrial-derived stromal cells to neural differentiation: In vitro and in vivo studies in rat. Journal of Biomedical Materials Research Part A
25. Tavakol S, Saber R, Hoveizi E, Tavakol B, Aligholi H, et al. (2015) Self-Assembling Peptide Nanofiber Containing Long Motif of Laminin Induces Neural Differentiation, Tubulin Polymerization, and Neurogenesis: In Vitro, Ex Vivo, and In Vivo Studies. Molecular neurobiology: 1–12
26. Tavakol S, Saber R, Hoveizi E, Aligholi H, Ai J, et al. (2015) Chimeric self-assembling nanofiber containing bone marrow homing peptide's motif induces motor neuron recovery in animal model of chronic spinal cord injury; an in vitro and in vivo investigation. Mol Neurobiol: 1–11
27. Hozumi K, Ishikawa M, Hayashi T, Yamada Y, Katagiri F et al (2012) Identification of cell adhesive sequences in the N-terminal region of the laminin α2 chain. J Biol Chem 287:25111–25122
28. Frith JE, Mills RJ, Hudson JE, Cooper-White JJ (2012) Tailored integrin–extracellular matrix interactions to direct human mesenchymal stem cell differentiation. Stem Cells Dev 21:2442–2456
29. Tysseling-Mattiace VM, Sahni V, Niece KL, Birch D, Czeisler C et al (2008) Self-assembling nanofibers inhibit glial scar formation and promote axon elongation after spinal cord injury. J Neurosc 28:3814–3823
30. Lampe KJ, Heilshorn SC (2012) Building stem cell niches from the molecule up through engineered peptide materials. Neurosci Lett 519:138–146
31. Takagi Y, Nomizu M, Gullberg D, MacKrell AJ, Keene DR et al (1996) Conserved neuron promoting activity in Drosophila and vertebrate laminin α1. J Biol Chem 271:18074–18081

32. Freitas VM, Vilas-Boas VF, Pimenta DC, Loureiro V, Juliano MA et al (2007) SIKVAV, a laminin α1-derived peptide, interacts with integrins and increases protease activity of a human salivary gland adenoid cystic carcinoma cell line through the ERK 1/2 signaling pathway. Am J Pathol 171:124–138
33. Maeda T, Titani K, Sekiguchi K (1994) Cell-adhesive activity and receptor-binding specificity of the laminin-derived YIGSR sequence grafted onto Staphylococcal protein A. J Biochem 115: 182–189
34. Boudreau N, Jones P (1999) Extracellular matrix and integrin signalling: the shape of things to come. Biochem J 339:481–488
35. Zhang X-M, Huang G-W, Tian Z-H, Ren D-L, Wilson JX (2009) Folate stimulates ERK1/2 phosphorylation and cell proliferation in fetal neural stem cells. Nutr Neurosci 12:226–232
36. Mruthyunjaya S, Rumma M, Ravibhushan G, Anjali S, Padma S (2011) c-Jun/AP-1 transcription factor regulates laminin-1-induced neurite outgrowth in human bone marrow mesenchymal stem cells: role of multiple signaling pathways. FEBS Lett 585:1915–1922
37. Ortinau S, Schmich J, Block S, Liedmann A, Jonas L et al (2010) Effect of 3D-scaffold formation on differentiation and survival in human neural progenitor cells. Biomed Eng Online 9:70
38. Zhang ZX, Zheng QX, Wu YC, Hao DJ (2010) Compatibility of neural stem cells with functionalized self-assembling peptide scaffold in vitro. Biotechnol Bioprocess Eng 15:545–551
39. Yang H, Qu T, Yang H, Wei L, Xie Z et al (2013) Self-assembling nanofibers improve cognitive impairment in a transgenic mice model of Alzheimer's disease. Neurosci Lett 556:63–68
40. Shaw D, Shoichet MS (2003) Toward spinal cord injury repair strategies: peptide surface modification of expanded poly (tetrafluoroethylene) fibers for guided neurite outgrowth in vitro. J Craniofacial Surg 14:308–316
41. Lévesque SG, Shoichet MS (2006) Synthesis of cell-adhesive dextran hydrogels and macroporous scaffolds. Biomaterials 27:5277–5285
42. Tavakol S, Aligholi H, Gorji A, Eshaghabadi A, Rezayat M et al (2015) P51: Thermogel nanofiber induces human endometrial-derived stromal cells to neural differentiation and improves motor dysfunction following spinal cord injury. Neurosci J Shefaye Khatam 2:101–101
43. Tavakol S, Saber R, Hoveizi E, Aligholi H, Ai J et al (2015) W6: Self-assembling peptide nanofiber containing biologic motif induces neural differentiation, tubulin polymerization and neurogenesis; in vitro, ex vivo and in vivo studies. Neurosci J Shefaye Khatam 2:49–49
44. Taraballi F, Natalello A, Campione M, Villa O, Doglia SM, et al. (2010) Glycine-spacers influence functional motifs exposure and self-assembling propensity of functionalized substrates tailored for neural stem cell cultures. Frontiers in neuroengineering 3
45. Wang H, Jin P, Sabatino M, Ren J, Civini S et al (2012) Comparison of endometrial regenerative cells and bone marrow stromal cells. J Transl Med 10:207
46. Han X, Meng X, Yin Z, Rogers A, Zhong J et al (2009) Inhibition of intracranial glioma growth by endometrial regenerative cells. Cell Cycle 8:606–610
47. Meng X, Ichim TE, Zhong J, Rogers A, Yin Z et al (2007) Endometrial regenerative cells: a novel stem cell population. J Transl Med 5:57
48. Lees JG, Lim SA, Croll T, Williams G, Lui S, et al. (2007) Transplantation of 3D scaffolds seeded with human embryonic stem cells: biological features of surrogate tissue and teratoma-forming potential
49. Tavakol S, Modarres Mousavi SM, Masummi M, Amani A, Rezayat SM, et al. (2014) The effect of Noggin supplementation in Matrigel nanofiber-based cell culture system for derivation of neural-like cells from human endometrial-derived stromal cells. Journal of Biomedical Materials Research Part A
50. Medistem (2011) Medistem receives FDA approval to begin clinical trial in USA with ERC stem cells. San Diego
51. Gelain F, Bottai D, Vescovi A, Zhang S (2006) Designer self-assembling peptide nanofiber scaffolds for adult mouse neural stem cell 3-dimensional cultures. PLoS ONE 1, e119
52. Ebrahimi-Barough S, Kouchesfehani HM, Ai J, Mahmoodinia M, Tavakol S et al (2013) Programming of human endometrial-derived stromal cells (EnSCs) into pre-oligodendrocyte cells by overexpression of miR-219. Neurosci Lett 537:65–70
53. Holtz A, Nyström B, Gerdin B (1989) Blocking weight-induced spinal cord injury in rats: effects of TRH or naloxone on motor function recovery and spinal cord blood flow. Acta Neurol Scand 80:215–220
54. Basso DM, Beattie MS, Bresnahan JC (1995) A sensitive and reliable locomotor rating scale for open field testing in rats. J Neurotrauma 12:1–21
55. Even-Ram S, Artym V, Yamada KM (2006) Matrix control of stem cell fate. Cell 126:645–647
56. Tashiro K-i, Sephel G, Weeks B, Sasaki M, Martin G et al (1989) A synthetic peptide containing the IKVAV sequence from the A chain of laminin mediates cell attachment, migration, and neurite outgrowth. J Biol Chem 264:16174–16182
57. Skubitz A, Letourneau PC, Wayner E, Furcht LT (1991) Synthetic peptides from the carboxy-terminal globular domain of the A chain of laminin: their ability to promote cell adhesion and neurite outgrowth, and interact with heparin and the beta 1 integrin subunit. J Cell Biol 115:1137–1148
58. Richard BL, Nomizu M, Yamada Y, Kleinman HK (1996) Identification of synthetic peptides derived from laminin α1 and α2 chains with cell type specificity for neurite outgrowth. Exp Cell Res 228:98–105
59. Cluzel C, Saltel F, Lussi J, Paulhe F, Imhof BA et al (2005) The mechanisms and dynamics of αvβ3 integrin clustering in living cells. J Cell Biol 171:383–392
60. Kim M, Carman CV, Yang W, Salas A, Springer TA (2004) The primacy of affinity over clustering in regulation of adhesiveness of the integrin αLβ2. J Cell Biol 167:1241–1253
61. Dupont S, Morsut L, Aragona M, Enzo E, Giulitti S et al (2011) Role of YAP/TAZ in mechanotransduction. Nature 474:179–183
62. Milewski RC, Chi NC, Li J, Brown C, Lu MM et al (2004) Identification of minimal enhancer elements sufficient for Pax3 expression in neural crest and implication of Tead2 as a regulator of Pax3. Development 131:829–837
63. Zhang H, Deo M, Thompson RC, Uhler MD, Turner DL (2012) Negative regulation of Yap during neuronal differentiation. Dev Biol 361:103–115
64. Keung AJ, de Juan-Pardo EM, Schaffer DV, Kumar S (2011) Rho GTPases mediate the mechanosensitive lineage commitment of neural stem cells. Stem Cells 29:1886–1897
65. Pla AF, Maric D, Brazer S-C, Giacobini P, Liu X et al (2005) Canonical transient receptor potential 1 plays a role in basic fibroblast growth factor (bFGF)/FGF receptor-1-induced Ca2+ entry and embryonic rat neural stem cell proliferation. J Neurosc 25: 2687–2701
66. Tai Y, Feng S, Du W, Wang Y (2009) Functional roles of TRPC channels in the developing brain. Pflügers Archiv-Eur J Physiol 458:283–289
67. Chan CE, Odde DJ (2008) Traction dynamics of filopodia on compliant substrates. Science 322:1687–1691
68. Defilippi P, Di Stefano P, Cabodi S (2006) p130Cas: a versatile scaffold in signaling networks. Trends Cell Biol 16:257–263
69. Sawada Y, Tamada M, Dubin-Thaler BJ, Cherniavskaya O, Sakai R et al (2006) Force sensing by mechanical extension of the Src family kinase substrate p130Cas. Cell 127:1015–1026
70. Buxbaum R, Heidemann S (1988) A thermodynamic model for force integration and microtubule assembly during axonal elongation. J Theor Biol 134:379–390

71. Ingber DE (2003) Tensegrity II. How structural networks influence cellular information processing networks. J Cell Sci 116:1397–1408
72. Dennerll T, Joshi H, Steel V, Buxbaum R, Heidemann S (1988) Tension and compression in the cytoskeleton of PC-12 neurites. II: Quantitative measurements. J Cell Biol 107:665–674
73. Iwashita M, Kataoka N, Toida K, Kosodo Y (2014) Systematic profiling of spatiotemporal tissue and cellular stiffness in the developing brain. Development 141:3793–3798
74. Lei Z-N, Liu F, Zhang L-M, Huang Y-L, Sun F-Y (2012) Bcl-2 increases stroke-induced striatal neurogenesis in adult brains by inhibiting BMP-4 function via activation of β-catenin signaling. Neurochem Int 61:34–42
75. Zhang R, Xue Y-Y, Lu S-D, Wang Y, Zhang L-M et al (2006) Bcl-2 enhances neurogenesis and inhibits apoptosis of newborn neurons in adult rat brain following a transient middle cerebral artery occlusion. Neurobiol Dis 24:345–356
76. Jiao J, Huang X, Feit-Leithman RA, Neve RL, Snider W et al (2005) Bcl-2 enhances Ca2+ signaling to support the intrinsic regenerative capacity of CNS axons. EMBO J 24:1068–1078
77. Hilton M, Middleton G, Davies AM (1997) Bcl-2 influences axonal growth rate in embryonic sensory neurons. Curr Biol 7:798–800
78. Wang Y, Sun Z-y, Zhang K-m, Xu G-q, Li G (2011) Bcl-2 in suppressing neuronal apoptosis after spinal cord injury. World J Emerg Med 2:38